Journal of Information Systems Engineering and Management
2025, 10(49s)
e-ISSN: 2468-4376
https://www.jisem-journal.com/

Research Article

Robust Control of PV Micro-Grids under Dynamic Conditions Using an Improved Nonlinear Fuzzy Logic Approach

Muhamad Nabil bin Hidayat*[1], Naeem Hannoon[2] , Rahimi bin Baharom[3] , Nor Farahaida Abdul Rahman[4], Wan Nor Aishah Binti Wan Abdul Munim[5], Mohd Talib Mat Yussoh[6]
[1,2,3,4,5,6]*Department of Electrical Engineering, Faculty of Electrical Engineering, Universiti Tecknologic Mara UiTM, Malaysia*

ARTICLE INFO

Received: 30 Dec 2024
Revised: 05 Feb 2025
Accepted: 25 Feb 2025

ABSTRACT

This study proposes a Modified Nonlinear Fuzzy Logic Controller (MNLC) as an advanced solution to improve load stability in photovoltaic (PV) micro-grid systems under challenging operational scenarios. Extensive simulations conducted in MATLAB Simulink benchmark the MNLC against the conventional Proportional-Integral (PI) controller under various disturbances such as high loading, symmetrical and asymmetrical faults, irradiance variability, and partial power shedding. Results reveal that the MNLC consistently outperforms the conventional controller by ensuring faster stabilization, minimizing transient oscillations, and optimizing solar energy harvesting. These findings underscore the MNLC's potential for enhancing the resilience and efficiency of PV-based distributed generation systems.

Keywords: Modified Nonlinear Fuzzy Controller, Photovoltaic Micro-grid, Load Stability, Renewable Energy, MATLAB Simulation.

INTRODUCTION

Photovoltaic (PV)-driven micro-grids play an increasingly vital role in promoting sustainable and decentralized energy solutions. However, maintaining robust operational stability amid dynamic environmental and load variations remains a formidable challenge. Conventional control methods, particularly Proportional-Integral (PI) controllers, offer satisfactory performance under steady-state conditions but often falter during transient disturbances where rapid adaptability is essential.

Given the heightened integration of intermittent PV resources, there is a growing demand for advanced controllers that can dynamically respond to fluctuations in irradiance, faults, and abrupt load changes. To address these challenges, this research introduces a Modified Nonlinear Fuzzy Logic Controller (MNLC) aimed at enhancing micro-grid stability, maximizing solar energy capture, and facilitating rapid recovery from disturbances. Unlike linear control schemes, fuzzy logic controllers offer inherent flexibility in managing the nonlinearities and uncertainties typical of renewable energy systems.

Building upon established PV system modeling frameworks, this study employs MATLAB Simulink to simulate a comprehensive range of operating conditions. Comparative evaluations between the MNLC and traditional PI controllers focus on critical performance indicators including stabilization time, power quality, fault resilience, and energy harvesting efficiency.

METHODOLOGY

System Model

System Modeling

The PV micro-grid is modeled using MATLAB Simulink, incorporating detailed parameters such as irradiance levels, load characteristics, and three-phase series RLC load specifications. The key simulation parameters are outlined in Table 1.

Journal of Information Systems Engineering and Management
2025, 10(49s)
e-ISSN: 2468-4376
https://www.jisem-journal.com/

Research Article

Table 1. Three-phase series RLC load parameter

Parameters	Value
Irradiance	1000
Three-Phase Load	
Nominal Vn(Vrms)	385
Nominal frequency fn(Hz)	60
Active power P(W)	1.00E+04
Inductive Reactive power Ql	2.00E+03
Capacitive Reactive power Qc	0

Controller Implementation

Controller Design and Implementation

The MNLC is designed and implemented alongside a conventional PI controller for benchmarking purposes. The control algorithms are tested under various scenarios including:

- High loading
- Symmetrical and asymmetrical faults
- Irradiance fluctuations
- Partial power shedding

Equations representing load dynamics and fault conditions are embedded within the simulation framework, ensuring realistic emulation of practical operating environments. Specifically, load power (P) is defined as:

$P = Vn \times I \times \cos(\varphi)$

where Vn denotes nominal voltage, I is current, and φ represents the power factor.

Figures and tables throughout the results section present the simulation outputs, enabling direct performance comparisons between the MNLC and the PI controller.

RESULTS AND DISCUSSION

Upon careful examination of the presented in Table2, and waveform data, a comprehensive analysis comparing the conventional controller and the Modified Non-Linear Fuzzy Controller (MNLC) in high loading conditions reveals significant insights. Notably, both controllers exhibit stable power waveforms without any visible ripples, indicating effective ripple mitigation capabilities.

Delving deeper into the data, it becomes apparent that the MNLC showcases an advantage as the MNLC outperforms the conventional controller in terms of stabilization time. The MNLC achieves steady-state load power in a swift 0.05s, whereas the conventional controller requires 0.153s. Similarly, for reactive power, the MNLC reaches stability in 0.05s, compared to the conventional controller's 0.153s. This notable difference in stabilization time further emphasizes the MNLC's superior responsiveness and its ability to adapt swiftly to high loading conditions. In terms of power values, the MNLC demonstrates higher solar power captured than the conventional ones which is observed at 9.56kW compared to the 7.56kW load and reactive power levels compared to its conventional counterpart. The load power value for the MNLC is recorded at 9.814kW, which is lower than the conventional controller's value of 34.4kW.

Similarly, the MNLC exhibits a reactive power value of 5.78kW, while the conventional controller registers 20.5kW.

Journal of Information Systems Engineering and Management
2025, 10(49s)
e-ISSN: 2468-4376
https://www.jisem-journal.com/

Research Article

High Loading Conditions Analysis

Under high loading conditions Fig 1, displays power waveforms for both controllers, and Table 2, shows the comparative results, emphasizing MNLC's faster stabilization times and higher solar power capture compared to the conventional controller. MNLC's advantages in load and reactive power stabilization further highlight its efficiency in managing power systems during high loading. Fig 1, shows the waveform of real and reactive power under high load conditions.

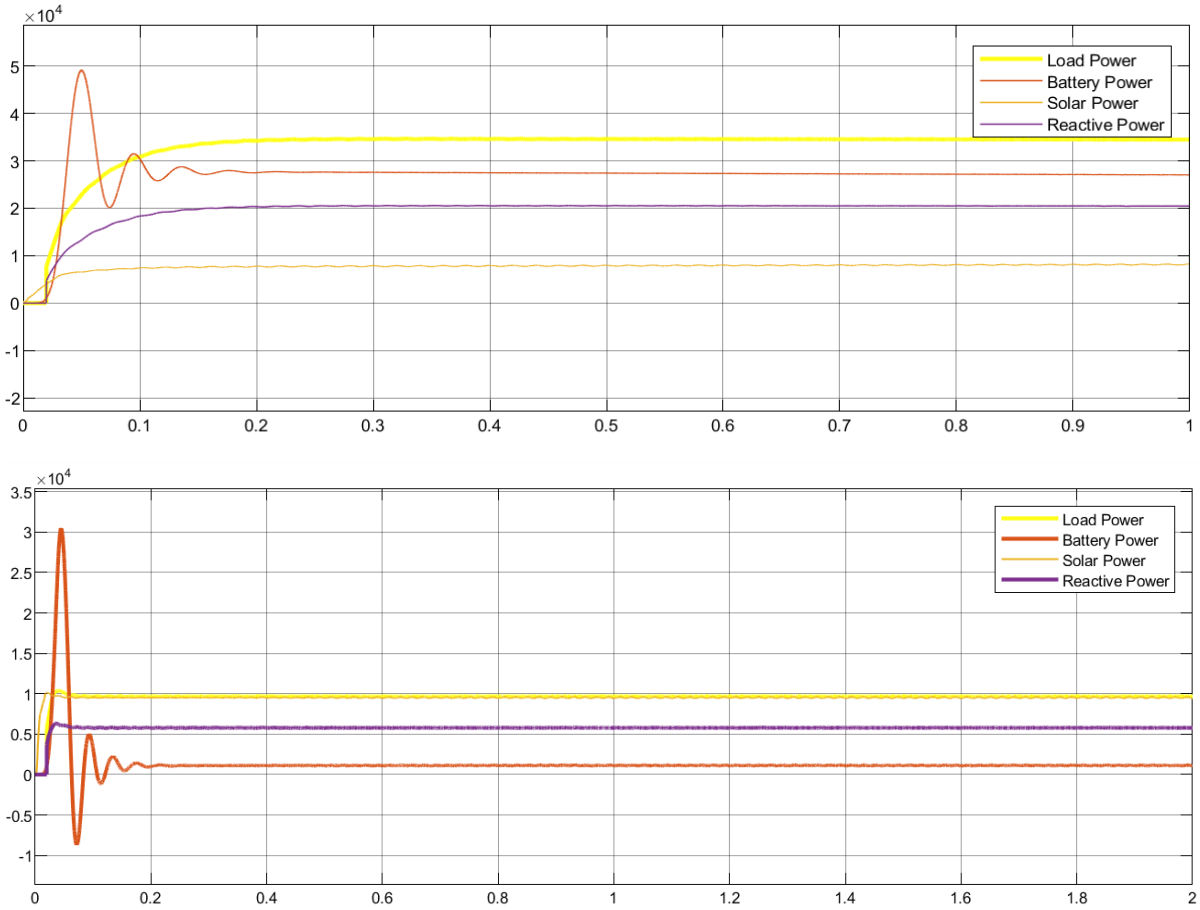

Figure 1. Power waveform for conventional controller (a) and Power waveform for MNLC (b)

Table 2. Result Value for High Loading Condition

High Loading Condition		Power Value (steady state)	Time to reach steady state
Load	Conventional	34.4kW	0.153s
	MNLC	9.814kW	0.05s
Solar	Conventional	7.56kW	0.153s
	MNLC	9.56kW	0.025s
Reactive	Conventional	20.5kW	0.153s
	MNLC	5.78kW	0.05s

In summary, the analysis of the table and waveform data underscores the advantages offered by the Modified Non-Linear Fuzzy Controller (MNLC) over the conventional controller in high loading scenarios. The MNLC not only maintains stable power waveforms without ripples but also exhibits higher solar power and faster stabilization

Journal of Information Systems Engineering and Management
2025, 10(49s)
e-ISSN: 2468-4376
https://www.jisem-journal.com/

Research Article

times. These findings position the MNLC as a highly efficient and reliable controller for managing power systems under high loading conditions, thereby contributing to improved system performance and stability.

Fault Conditions Analysis

Fig 2, displays a symmetrical fault management unit that includes a time module. This module is essential for controlling the response of the solar energy installation during network faults. It has been optimized based on various conditions [4] to ensure efficient operation.

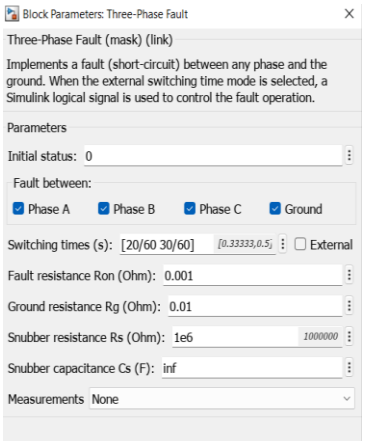

Figure 2. Fault Parameters for 3 Line Ground (symmetrical fault)

Fig 3, (a) and (b) show cases the waveform analysis of the symmetrical fault, specifically the 3-line Ground fault. These waveforms visually represent the electrical characteristics and behaviour associated with the fault. Moreover, they allow for a comparative assessment of the performance between the conventional controller and the proposed modified non-linear fuzzy controller. By analyzing these waveforms, the effectiveness of each controller in managing the system dynamics can be evaluated when confronted with this type of fault condition**.**

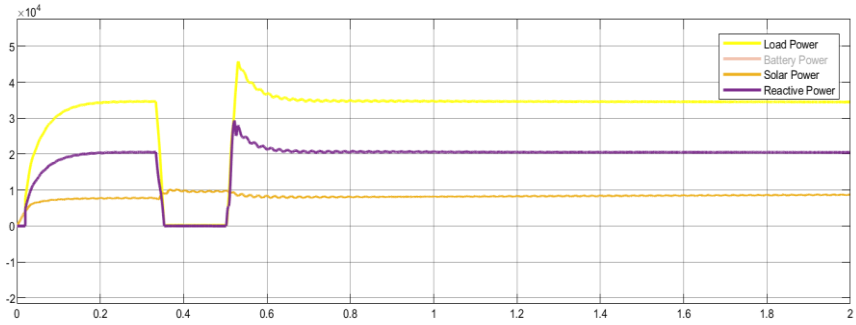

(a)

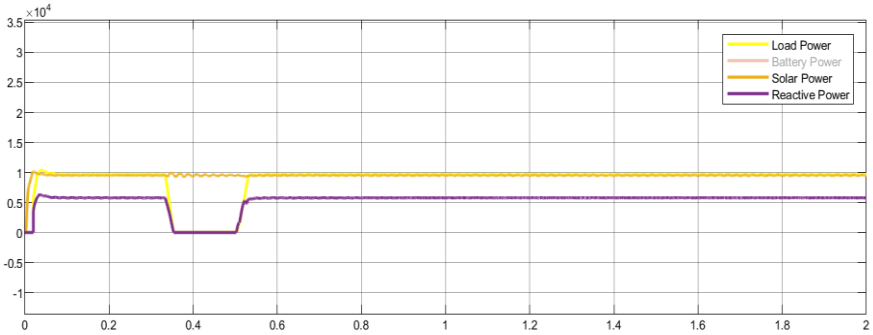

(b)

Figure 3. Symmetrical fault condition for conventional controller (a) and Fault condition for MNLC (b)

Journal of Information Systems Engineering and Management
2025, 10(49s)
e-ISSN: 2468-4376
https://www.jisem-journal.com/

Research Article

Table 3. Result value for Symmetrical Fault Condition

Symmetrical Fault Condition		Power Value (steady state)	Power Value (During Fault)	Stabilisation Time during fault
Load	Conventional	34.5kW	0.19kW	0.356s
	MNLC	9.7kW	0.05kW	0.205s
Solar	Conventional	7.623kW	9.45kW	0.267s
	MNLC	9.56kW	9.522kW	N/A
Reactive	Conventional	20.5kW	0.003kW	0.314s
	MNLC	5.82kW	-0.03kW	0.223s

Results for symmetrical faults Table 3, two-line ground faults Table 4, and line ground faults Table 5, emphasize MNLC's superior stability and reduced power fluctuations compared to the conventional controller. MNLC consistently outperforms in terms of stabilization time and managing power during fault conditions.

The comparative analysis between Conventional Controllers (CC) and Modified Nonlinear Fuzzy Controllers (MNLC) during symmetrical 3-Line Ground Fault (3LGF) conditions unveils intriguing disparities in their performance. MNLC demonstrates a longer stabilization time during fault conditions, needing 0.205s to stabilize load power compared to CC's 0.356s, and 0.223s compared to CC's 0.314s for reactive power. This indicates that MNLC requires more time to regain stability during faults. Notably, when examining solar power waveforms, CC exhibits an increase from 7.623kW to 9.45kW during faults, while MNLC maintains a constant power level of 9.56kW. This suggests that MNLC ensures a consistent solar power output during fault conditions, whereas CC encounters fluctuations in power demand. Regarding load power behaviour, CC experiences a dip during the fault followed by spikes surpassing the steady-state power of 34.5kW. In contrast, MNLC only experiences a dip from 9.7kW to 0.05kW without subsequent spikes, eventually returning to the steady-state power. This highlights MNLC's ability to facilitate a smoother transition in load power during fault conditions, minimizing abrupt fluctuations. Furthermore, CC displays ripples in load and reactive power during post-fault recovery, whereas MNLC exhibits a more stable response. These findings underscore the superior performance of MNLC in maintaining stability and reducing power fluctuations during symmetrical 3LGF conditions [5].

Two Line Ground Fault and Line Ground Fault

In this study, an analysis is presented for fault parameters of two distinct types of unsymmetrical faults: the 2 Line-Ground fault and Line-Ground fault. The fault parameters specific to each type are depicted in Fig 4, and 6, respectively. Valuable insights into the unique characteristics associated with each unsymmetrical fault scenario are provided by these figures.

Journal of Information Systems Engineering and Management
2025, 10(49s)
e-ISSN: 2468-4376
https://www.jisem-journal.com/

Research Article

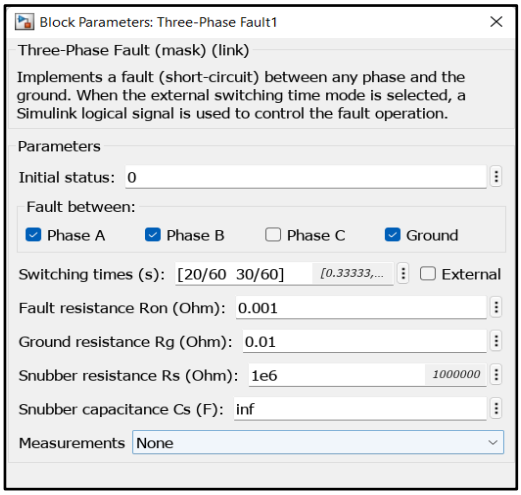

Figure 4. Fault Parameters for 2-Line Ground Fault Condition

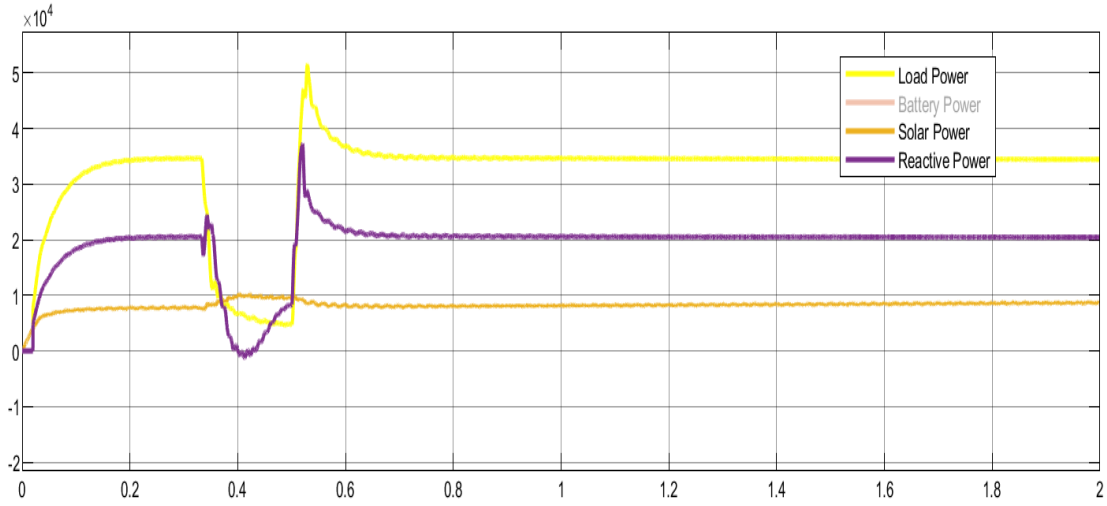

(a)

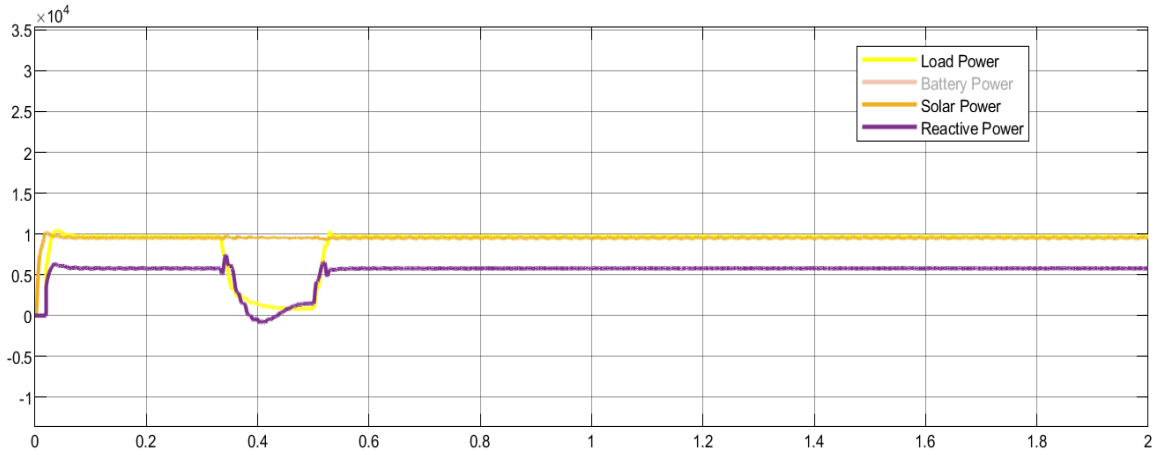

(b)

Figure 5. 2-Line Ground fault condition for conventional controller (a) and Fault condition for MNLC (b)

Journal of Information Systems Engineering and Management
2025, 10(49s)
e-ISSN: 2468-4376
https://www.jisem-journal.com/

Research Article

Furthermore, the power waveforms observed during these unsymmetrical fault conditions are examined. Specifically, the power waveforms for the 2 Line-Ground fault and Line-Ground fault are showcased in Fig 5, and 7, respectively. Additionally, the Result Value for the 2-Line Ground Fault Condition and Line-Ground Fault Condition is also presented in Table 4, and Table 5, respectively.

Table 4. Result Value for 2-Line Ground Fault Condition.

2-Line Ground Fault Condition		Power Value (steady state)	Power Value (During Fault)	Stabilisation Time during fault
Load	Conventional	34.5kW	5.46kW	0.340s
	MNLC	9.7kW	1.08kW	0.198s
Solar	Conventional	7.623kW	9.82W	0.309s
	MNLC	9.56kW	9.582kW	N/A
Reactive	Conventional	20.5kW	1.50kW	0.331s
	MNLC	5.82kW	-0.47kW	0.198s

Table 5. Result Value for Line Ground Fault Condition

1 Line Ground Fault Condition	Power Value (steady state)	Power Value (During Fault)	Stabilisation Time during fault
Load	Conventional	34.5kW	19.6kW	0.345s
	MNLC	9.7kW	5.33kW	0.198s
Solar	Conventional	7.623kW	8.925kW	0.289s
	MNLC	9.56kW	9.58kW	N/A
Reactive	Conventional	20.5kW	49.8kW	0.337s
	MNLC	5.82kW	9.037kW	0.198s

Low and High Resistance Faults Analysis

MNLC excels in handling low and high resistance faults Tables 6 and 7, by achieving faster stabilization and minimizing power fluctuations. The analysis underscores the significance of fault resistance in grid-connected PV systems and the superior performance of MNLC in such scenarios.

In the context of Line-Ground Fault scenarios, Fig 8 and 10, present crucial parameters pertaining to low and high resistance faults. Additionally, Fig 9 and 11, exhibit a comparative analysis between a conventional control system and a proposed controller simulation, specifically focusing on their performance variation when subjected to different fault resistance conditions. Notably, the fault resistance values are intentionally adjusted to evaluate their impact on the overall system performance [6]. For instance, the high resistance fault condition involves modifying the fault resistance from its default value of 0.001 ohm to 0.2 ohm. Similarly, the low resistance fault condition considers a fault resistance adjustment to 0.0001 ohm which is lower than the default settings of simulation fault block. These figures offer valuable insights into the contrasting performance outcomes observed between the conventional control system and the proposed controller when exposed to diverse fault resistance scenarios.

Journal of Information Systems Engineering and Management
2025, 10(49s)
e-ISSN: 2468-4376
https://www.jisem-journal.com/

Research Article

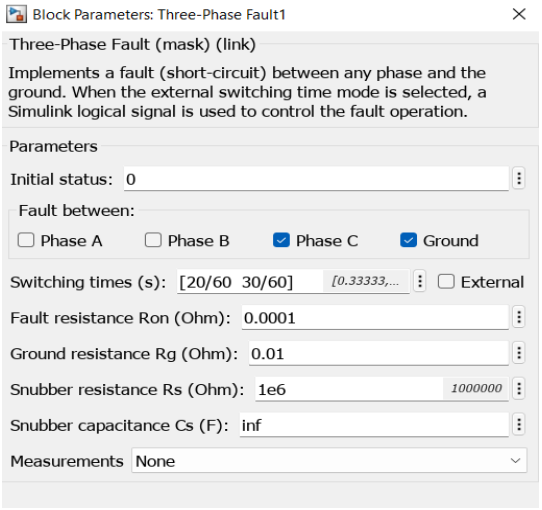

Figure 6. Parameters for low resistance fault condition

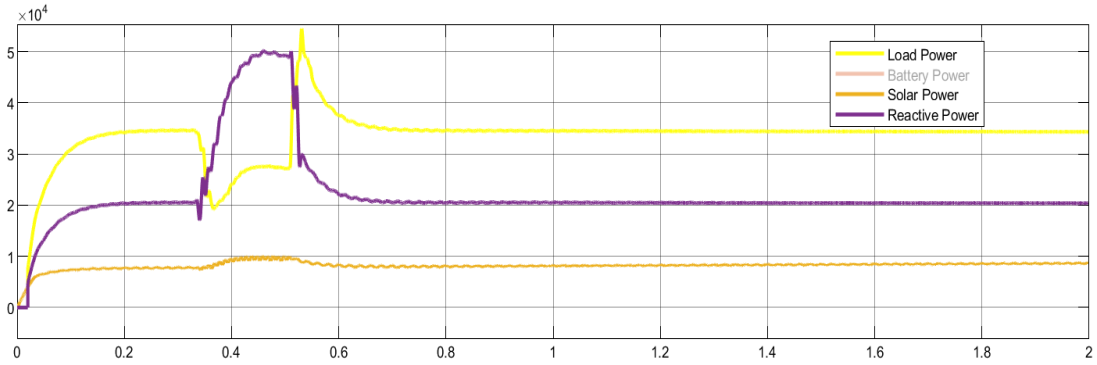

(a)

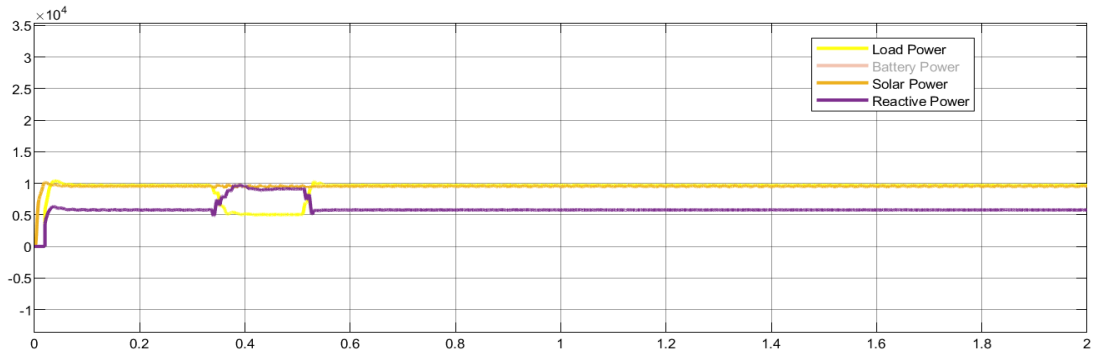

(b)

Figure 7. Low resistance fault condition for conventional controller (a) and Fault condition for MNLC (b)

Table 6. Result Value for Low Resistance Fault Condition

Low Resistance Fault Condition		Power Value (steady state)	Power Value (During Fault)	Duration for system to stabilize to steady state
Load	Conventional	34.5kW	19.6kW	0.345s

Journal of Information Systems Engineering and Management
2025, 10(49s)
e-ISSN: 2468-4376
https://www.jisem-journal.com/

Research Article

	MNLC	9.7kW	5.33kW	0.198s
Solar	Conventional	7.623kW	8.925kW	0.289s
	MNLC	9.56kW	9.58kW	N/A
Reactive	Conventional	20.5kW	49.8kW	0.337s
	MNLC	5.82kW	9.037kW	0.198s

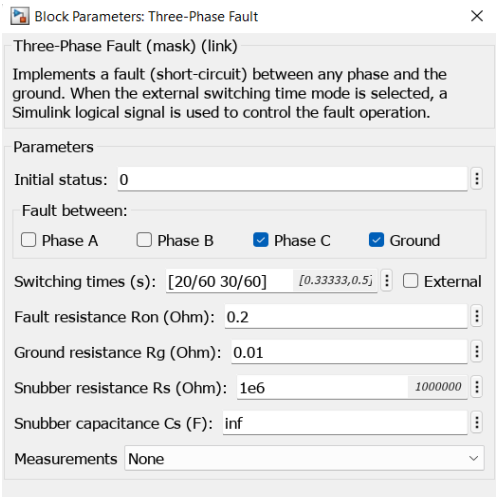

Figure 8. Parameters for high resistance fault condition

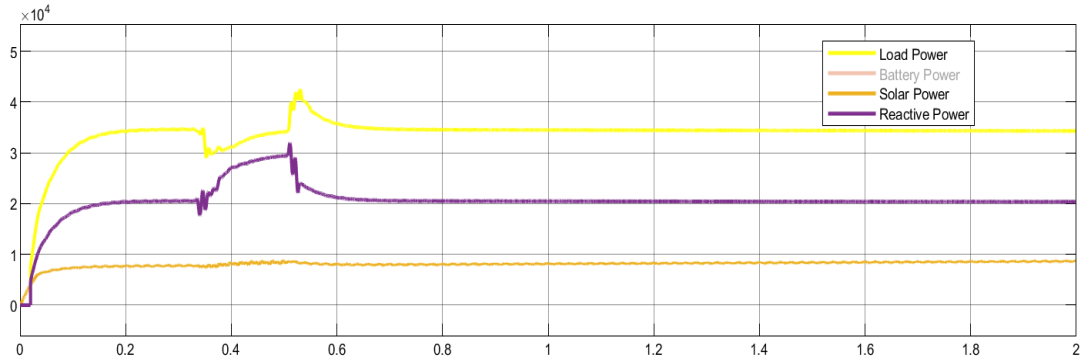

(a)

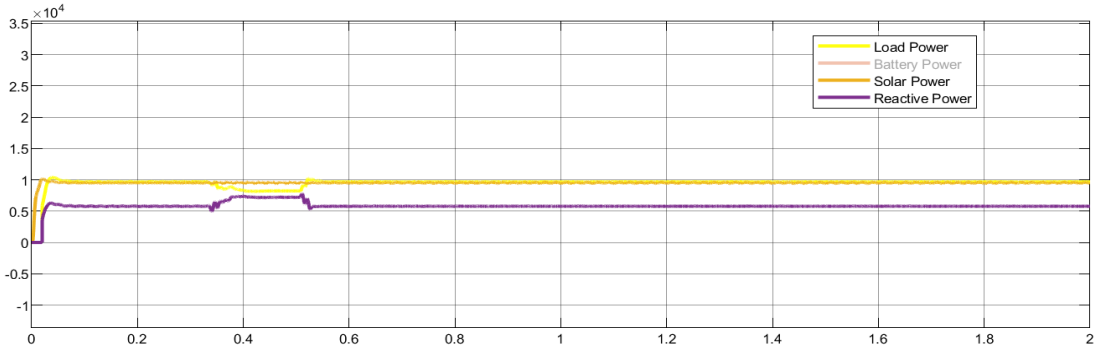

(b)

Figure 9. High resistance fault condition for conventional controller (a) and Fault condition for MNLC (b)

Journal of Information Systems Engineering and Management
2025, 10(49s)
e-ISSN: 2468-4376
https://www.jisem-journal.com/

Research Article

Table 1. Result value high resistance fault condition.

High Resistance Fault Condition		Power Value (steady state)	Power Value (During Fault)	Time Duration for system to stabilize to steady state
Load	Conventional	34.5kW	19.6kW	0.345s
	MNLC	9.7kW	5.33kW	0.198s
Solar	Conventional	7.623kW	8.925kW	0.289s
	MNLC	9.56kW	9.58kW	N/A
Reactive	Conventional	20.5kW	49.8kW	0.337s
	MNLC	5.82kW	9.037kW	0.198s

Under both the Low Resistance Fault and High Resistance Fault conditions, a comparative analysis was conducted to evaluate the performance of the Conventional Controller (CC) and the Modified Non-Linear Fuzzy Controller (MNLC). In a grid-connected photovoltaic (GCPV) system, fault resistance plays a crucial role during fault conditions, such as short circuits. It refers to the electrical resistance present in the system, helping to limit the current flow and prevent damage to the electrical components, as well as reduce the risk of fire [7]. The value of the waveform under the Low Resistance Fault and High Resistance Fault has been tabulated in Table 6 and Table7, respectively, providing further insights into the behaviour and response of both controllers in these fault condition.

In the Low Resistance Fault scenario, the MNLC demonstrated faster stabilization time, with a duration of 0.198s compared to the CC's 0.345s. The MNLC also maintained a constant solar power output (9.56kW and 9.58kW) during the fault, while the CC experienced fluctuations. Additionally, the MNLC exhibited smoother waveforms with reduced ripples, indicating more stable power output. Both controllers showed higher reactive power values compared to load power during the fault, but the CC experienced a significant spike (49.8kW) before returning to steady state, while the MNLC showed a smoother transition. These findings highlight the advantages of the MNLC, including faster stabilization, constant solar power output, reduced ripples, and effective management of reactive power during low resistance fault conditions [8].

Similarly, in the High Resistance Fault analysis, the CC experienced a decrease in load power from 34.5kW to 19.6kW during the fault, stabilizing in approximately 0.345 seconds, while the MNLC showed a lower load power value of 9.7kW, stabilizing in just 0.198 seconds. The CC's solar power output decreased from 7.623kW to 8.925kW during the fault, with a stabilization time of 0.289 seconds, while the MNLC maintained a constant solar power output of 9.56kW. The CC exhibited a significant increase in reactive power (20.5kW to 49.8kW) before stabilization, while the MNLC showed a lower reactive power value of 5.82kW, rising slightly to 9.037kW. The CC's waveforms displayed dips, spikes, and ripples in load power, prominent spikes and ripples in reactive power, and fluctuations in solar power. In contrast, the MNLC demonstrated a more stable response with minimal disturbances, including a slight dip in load power, a small rise in reactive power without spikes, and minimal ripples in the waveforms.

These findings not only highlight the superior performance of the MNLC in managing high resistance faults but also emphasize the significance of fault resistance in GCPV systems. Fault resistance plays a crucial role in limiting current flow, ensuring system safety, and preventing damage to components. Furthermore, appropriate fault protection devices, such as fuses or circuit breakers, are recommended to interrupt current flow and enhance system reliability. By considering fault resistance and employing reliable fault protection mechanisms, GCPV systems can achieve efficient and stable performance under various fault conditions.

Journal of Information Systems Engineering and Management
2025, 10(49s)
e-ISSN: 2468-4376
https://www.jisem-journal.com/

Research Article

Irradiance Conditions Analysis

Under varying irradiance conditions Tables 8 and 9, MNLC exhibits superior solar power generation and faster stabilization times compared to the conventional controller. MNLC's ability to optimize solar power utilization is emphasized, reinforcing its effectiveness in grid-connected PV systems.

A comparison between the Conventional Controller and the Modified Non-Linear Fuzzy Controller was conducted under different irradiance conditions. Figures depicting the performance of these controllers were included, showcasing the effects of irradiance levels of 500 and 1600 on Load, Reactive, and Solar Power. The intention was to observe and analyze how the controllers respond to varying irradiance levels, providing valuable insights into their behaviour.

In a partial shedding scenario was introduced to further investigate the system's behaviour. This involved applying a dynamic change in irradiance from 1000 to 650 over a time span of 0 to 2 seconds. By closely examining the system's response during this scenario, a more comprehensive understanding of the controllers' performance under such conditions was achieved.

Throughout the simulation, meticulous data collection was conducted, and the observations and measurements were carefully tabulated. The waveform outputs and power variations under different irradiance conditions were thoroughly analyzed. This analysis allows for a detailed assessment of the performance and effectiveness of both the Conventional Controller and the Modified Non-Linear Fuzzy Controller in managing and adapting to varying levels of irradiance.

Irradiance 500 and 1600

Fig11 and 13 provide insights into the performance of both the Conventional Controller (CC) and the Modified Non-Linear Fuzzy Controller (MNLC) when confronted with different irradiance conditions.

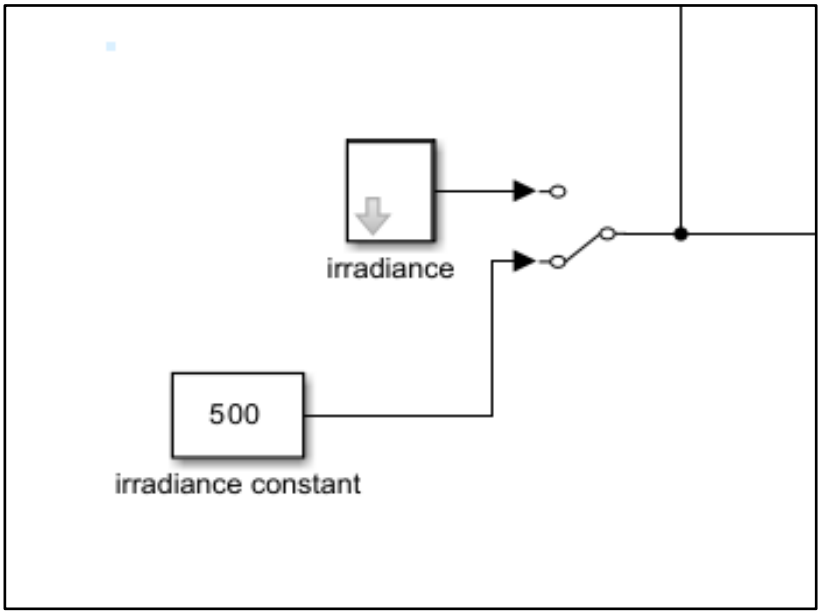

Figure 10. Parameters block for irradiance 500.

Journal of Information Systems Engineering and Management
2025, 10(49s)
e-ISSN: 2468-4376
https://www.jisem-journal.com/

Research Article

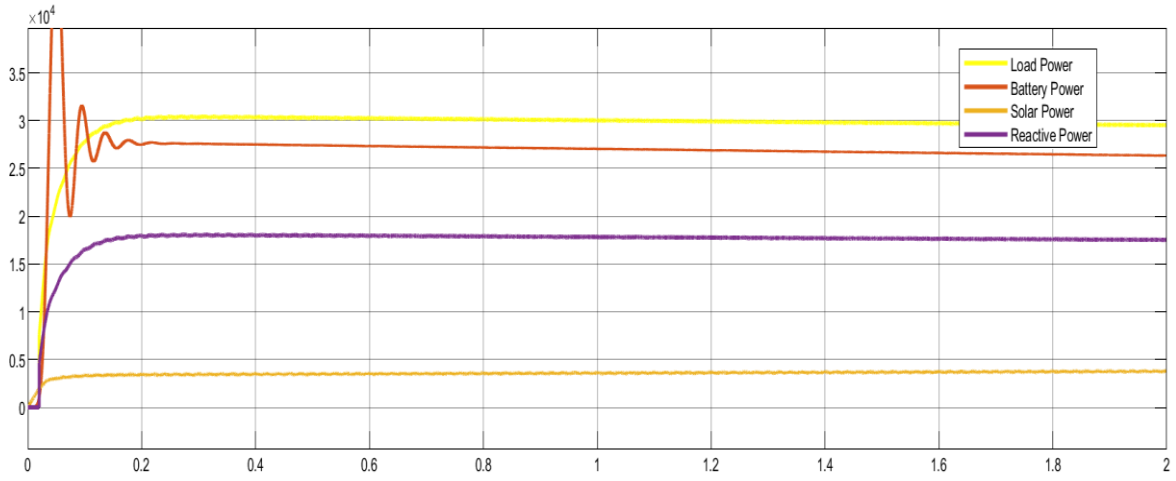

(a)

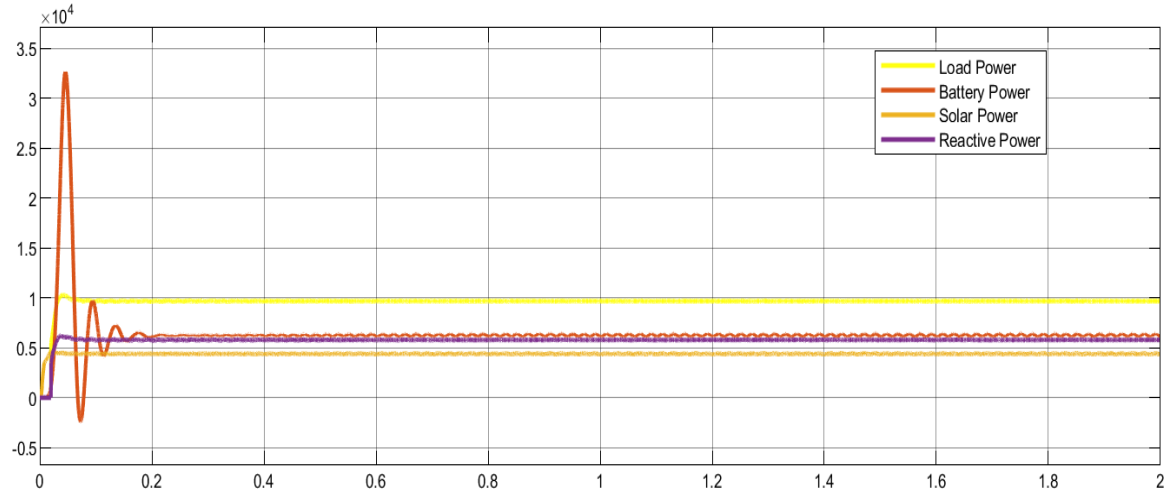

(b)

Figure 11. Irradiance 500 condition for conventional controller (a)and Irradiance 500 condition for MNLC (b)

Table 1. Results value for irradiance 500

Irradiance 500 condition		Power Value (steady state)	Time to steady state
Load	Conventional	30.4kW	0.173s
	MNLC	9.7kW	0.061s
Solar	Conventional	3.40kW	0.048s
	MNLC	4.40kW	0.025s
Reactive	Conventional	18.1kW	0.175s
	MNLC	5.76kW	0.046s

Journal of Information Systems Engineering and Management
2025, 10(49s)
e-ISSN: 2468-4376
https://www.jisem-journal.com/

Research Article

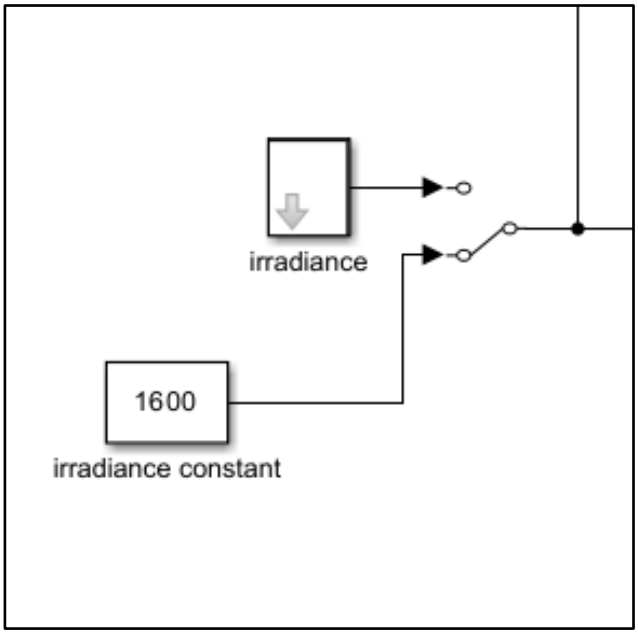

Figure 1. Parameters block for irradiance 1600.

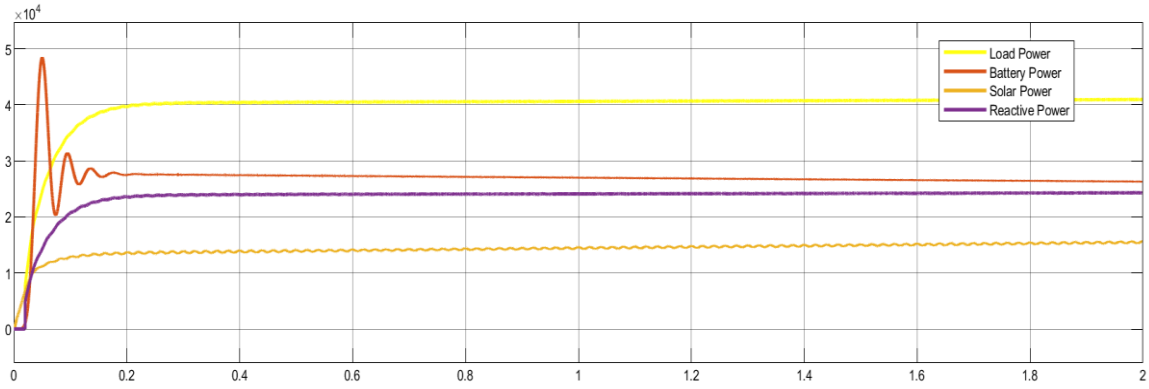

(a)

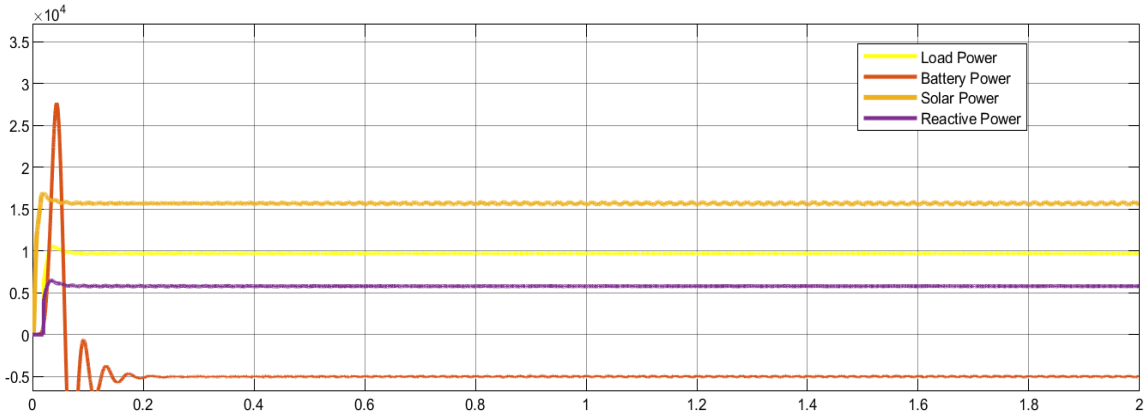

(b)

Figure 1. Irradiance 1600 condition for conventional controller (a) and Irradiance. 1600 condition for MNLC (b)

Journal of Information Systems Engineering and Management
2025, 10(49s)
e-ISSN: 2468-4376
https://www.jisem-journal.com/

Research Article

Table 1. Results value for irradiance 1600

Irradiance 1600 condition		Power Value (steady state)	Time to steady state
Load	Conventional	39.4kW	0.173s
	MNLC	9.72kW	0.061s
Solar	Conventional	13.6kW	0.048s
	MNLC	15.87kW	0.025s
Reactive	Conventional	23.77kW	0.175s
	MNLC	5.76kW	0.046s

The comparison between the Conventional Controller (CC) and the Modified Non-Linear Fuzzy Controller (MNLC) under different irradiance conditions reveals interesting findings, particularly in terms of the optimum solar power achieved by the MNLC compared to the CC.

Under the Irradiance 500 condition which is established based on Fig14, the MNLC demonstrates superior performance in maintaining a higher steady-state solar power output. Referring to Table 9, while the CC reaches a steady state of 3.40kW, the MNLC achieves an impressive 4.40kW, indicating its ability to harness and utilize solar energy more efficiently. Additionally, the MNLC exhibits a significantly shorter time to reach steady state, taking only 0.025s compared to the CC's 0.048s.

Similarly, under the Irradiance 1600 condition, the MNLC continues to outperform the CC in terms of solar power generation. While the CC reaches a steady state of 13.6kW, the MNLC achieves an even higher value of 15.87kW. This substantial difference further emphasizes the MNLC's capability to optimize solar power utilization. Notably, the MNLC again showcases a faster time to steady state, taking 0.025s compared to the CC's 0.048s.

Interestingly, despite the differences in irradiance levels, the load power remains consistent for both controllers in both situations. This indicates that the load power is not directly influenced by changes in irradiance and is effectively regulated by the controllers. Therefore, the MNLC's superior performance in achieving optimal solar power output does not impact the load power stability [9].

In summary, the analysis highlights the MNLC's remarkable ability to maximize solar power generation, surpassing the CC in both Irradiance 500 and Irradiance 1600 conditions. The MNLC achieves higher steady-state solar power values and exhibits faster stabilization times, indicating its efficiency and effectiveness in adapting to varying irradiance levels. These findings further support the advantage of employing the MNLC as a controller to enhance solar power utilization and system performance in grid-connected photovoltaic systems.

Partial Shedding Analysis

MNLC outperforms the conventional controller during partial shedding Table10. by maintaining stable load and reactive power, as well as consistently achieving higher solar power output. The results highlight MNLC's efficiency in adapting to changing irradiance conditions.

The analysis of the partial shedding scenario provides valuable insights into how the Conventional Controller (CC) and the Modified Non-Linear Fuzzy Controller (MNLC) perform under changing irradiance conditions [10].

Journal of Information Systems Engineering and Management
2025, 10(49s)
e-ISSN: 2468-4376
https://www.jisem-journal.com/

Research Article

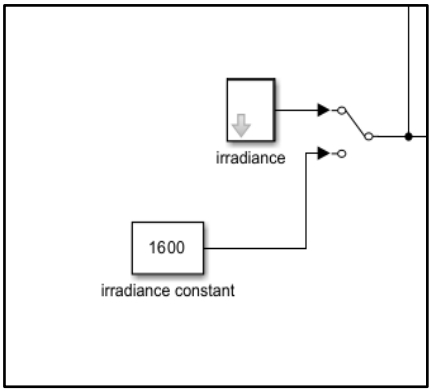

Figure 1. Parameters block for partial shedding.

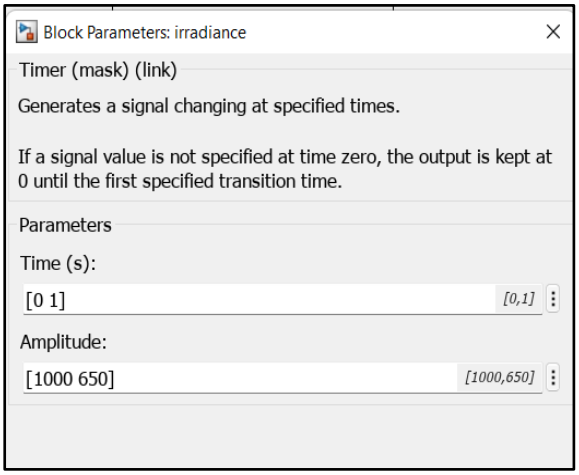

Figure 1. Parameters value applied for partial shedding.

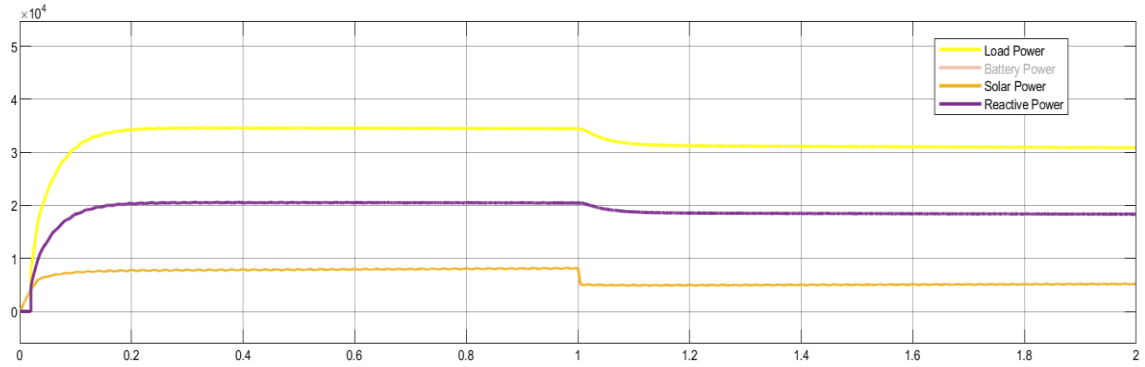

(a)

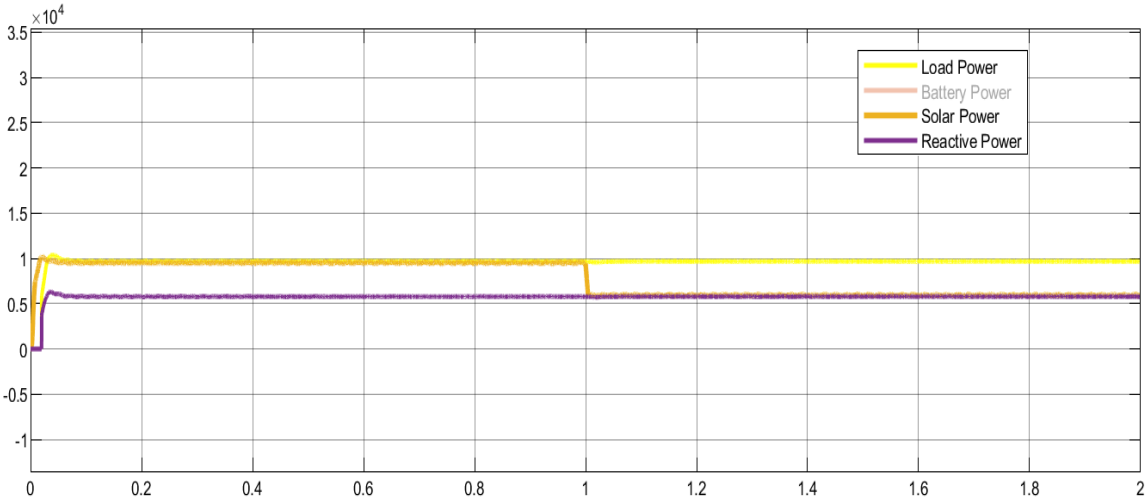

(b)

Figure 16. Partial shedding condition for conventional controller (a) and partial shedding condition for MNLC (b)

Journal of Information Systems Engineering and Management
2025, 10(49s)
e-ISSN: 2468-4376
https://www.jisem-journal.com/

Research Article

Table 1 Results value for Partial Sheddin

Partial Shedding Condition		Power Value (Steady state) at 0-1s, 1000 irradiance	Power Value (Steady state) at 1-2s, 650 irradiances
Load	Conventional	39.4kW	31.2kW
	MNLC	9.72kW	9.78kW
Solar	Conventional	7.91kW	5.023kW
	MNLC	9.53kW	5.99kW
Reactive	Conventional	23.77kW	18.53kW
	MNLC	5.76kW	5.76kW

When irradiance is low, the MNLC does a great job of adjusting the output power of the grid-connected PV system. It does this by regulating the DC-DC converter and inverter, which helps maintain stable and efficient system operation. The controller also tweaks the maximum power point tracking (MPPT) data, ensuring that the PV system operates at its best point and extracts more energy from the PV modules during low irradiance conditions. It's worth noting that the same positive outcome holds true even when irradiance is high. The MNLC can track system parameters such as DC current and voltage, ensuring stable performance. Additionally, it has the ability to limit the power output of the PV system to avoid overloading the grid and ensure compliance with grid codes and regulations.

The partial shedding scenario according to Table10, the MNLC manages to maintain a consistent load power and reactive power throughout the transition. The load power remains steady at 9.72kW during the first second and only slightly increases to 9.78kW from 1-2 seconds. Similarly, the reactive power stays constant at 5.76kW throughout the partial shedding period for the MNLC. This shows us that the MNLC has the knack for regulating and stabilizing the load and reactive power, even when faced with changing irradiance conditions.

In contrast, the CC experiences a reduction in load power from 39.4kW to 31.2kW during the initial second of partial shedding. It's interesting to note that the load power for the CC takes some time to adjust and reach a steady state value of 31.2kW. The CC's solar power output is also affected by the change in irradiance, dropping from 7.91kW to 5.023kW during the first second. Additionally, the CC's reactive power undergoes a reduction from 23.77kW to 18.53kW. These changes in power values indicate that the CC requires more time to adjust and stabilize its power outputs during partial shedding.

One notable aspect is that the MNLC consistently outperforms the CC when it comes to solar power generation in all scenarios. Even during partial shedding, the MNLC manages to maintain a higher steady-state solar power output compared to the CC. Specifically, the MNLC achieves 9.53kW of solar power during the initial second and further increases it to 5.99kW from 1-2 seconds. This clearly demonstrates the MNLC's effectiveness in efficiently harnessing and utilizing solar energy, surpassing the CC in maintaining a steady and optimal solar power output under partial shedding conditions.

To sum it up, the analysis highlights the advantages of using the MNLC in partial shedding scenarios. It maintains stable load and reactive power, whereas the CC experiences reductions in load, solar, and reactive power during the transition. Furthermore, the MNLC consistently achieves higher solar power output compared to the CC, which indicates its superior performance and effectiveness in managing changing irradiance conditions. The MNLC's ability to adjust output power, optimize the MPPT data, and track system parameters ensures stable operation and compliance with grid codes and regulations, preventing any grid overloading concerns [11].

Journal of Information Systems Engineering and Management
2025, 10(49s)
e-ISSN: 2468-4376
https://www.jisem-journal.com/

Research Article

Small Signal Stability Analysis

Analysis of the Bode plot and Nyquist diagram Fig17 indicates that MNLC exhibits larger gain and phase margins, demonstrating improved stability compared to the conventional controller. MNLC's responsiveness and stability are further validated through these graphical representations.

The Bode plot and Nyquist diagram in Fig19 provide a means to compare the conventional PV controller and the proposed controller in terms of stability and performance.

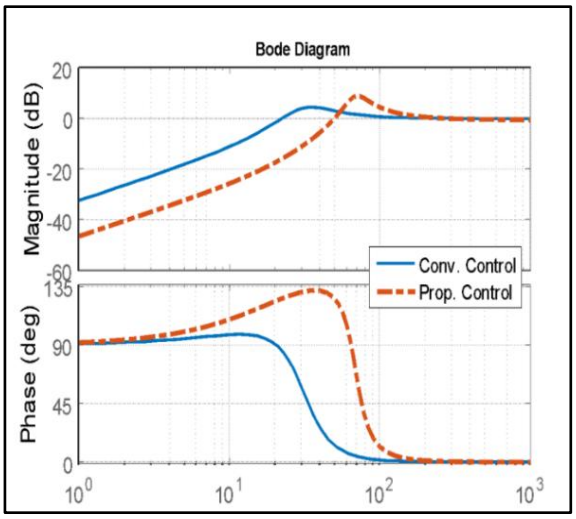

(a)

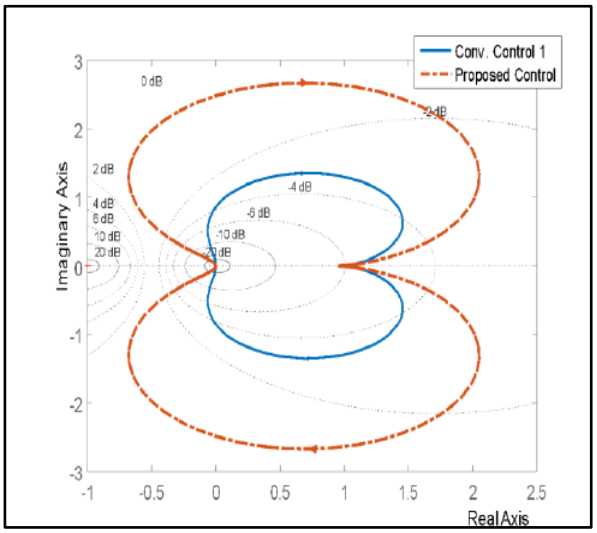

(b)

Figure 17. Small signal stability: Bode plot (a), Nyquist diagram (b)

Analyzing the Bode plot reveals that the proposed controller exhibits larger gain and phase margins than the conventional controller, indicating improved stability. This means that the proposed controller is more resilient to disturbances and uncertainties, making it a more stable option.

Examining the Nyquist diagram offers further insights. The proposed controller, known as MNLC, demonstrates a larger stability margin, fewer encirclements of the critical point, and closed loop poles closer to the left half plane compared to the conventional controller. These traits demonstrate that the proposed controller surpasses the conventional one in terms of responsiveness and stability. It has a wider range of system variation tolerance, a more stable and well-behaved response with fewer oscillations, and faster response times.

In conclusion, based on the analysis of the Bode plot and Nyquist diagram, the proposed controller shows superior stability characteristics with larger gain and phase margins. The Nyquist diagram confirms its better performance with a larger stability margin, fewer encirclements of the critical point, and closed-loop poles positioned closer to the left half plane. Therefore, the proposed controller demonstrates improved response and stability when compared to the conventional PV controller.

CONCLUSION

This study presented a comprehensive comparative analysis of a Modified Nonlinear Fuzzy Logic Controller (MNLC) against a conventional Proportional-Integral (PI) controller for stability enhancement in photovoltaic (PV) micro-grid systems. Extensive simulations under diverse operational scenarios — including high loading, symmetrical and asymmetrical faults, irradiance variations, and partial power shedding — demonstrated that the MNLC consistently outperforms the conventional approach.

The MNLC exhibited significantly faster stabilization times, improved solar power capture, minimized transient oscillations, and greater fault resilience. Moreover, the controller maintained superior system performance even under severe disturbances, achieving smoother power regulation and enhanced energy harvesting efficiency. These results affirm the MNLC's potential to enhance the reliability, adaptability, and operational quality of future PV-based distributed generation systems.

Future Work: Further research is recommended to validate the MNLC's performance through real-world experimental implementations and to explore the integration of adaptive machine learning techniques for dynamic tuning of the fuzzy logic parameters in larger, interconnected smart grid networks.

REFERENCES

[1] Youssef Elomari, Masoud Norouzi,“ Integration of Solar Photovoltaic Systems into Power Networks,” A Scientific Evolution Analysis. In Sustainable Development of Solar Photovoltaic Islands,Decarbonization 14(15),2022, 9249; https://doi.org /10.3390/su14159249.

[2] Zdenko Kovacic, Stjepan Bogdan,“Fuzzy Controller Design Theory and Application“, Publisher CRC Press – Taylor&Francis ISBN: 9781315221144,2006, https://doi.org /10.1201/9781420026504.

[3] Marcelo Gradella Villalva, Jonas Rafael Gazoli.,“Modeling and circuit-based simulation of photovoltaic arrays“, Conference Power Electronics Conference COBEP '09. Brazilian. https://doi.org/10.1109/COBEP.2009.5347680.

[4] Vinoliney, M. Lydia, and Y. Levron, “Optimal Grid Integration of renewable energy sources with energy storage using DQ0 based Inverter Controller “, International Conference on Inventive Computation Technologies (ICICT) , 2020.

[5] Saif Ul Islam, Soobae Kim, “ Design of an Optimal Adoptive Fault Ride through Scheme for Overcurrent Protection of Grid-Forming Inverter-Based Resources under Symmetrical Faults“, Published in Recent Advancements in Renewable Energy and Electrical Power Engineering Technology. https://doi.org /10.3390/su15086705.2023.

[6] D. Filomena, “Fault Resistance Influence on Faulted Power Systems with Distributed Generation“, Presented at the International Conference on Power Systems Transients (IPST'07) in Lyon, France on June 4-7.2007.

[7] Z. Hassan,A. Amir,Jeyraj Selvaraj, “A review on current injection techniques for low-voltage ride-through and grid fault conditions in grid-connected photovoltaic system “, Solar Energy 207(47):851-873,2020, https://doi.org / 10.1016/j.solener.

[8] Abdul Kadir, A.F Mupangat, H.,Mat Said, D., &Rasin, Z,”Reactive Power Analysis at Solar Power Plant”,Journal Teknologi, 83(2),47–https://doi.org/10.11113/jurnalteknologi.v83.15104, 2021.

[9] Mohsen Taherbaneh, A. H. Rezaie, H. Ghafoorifard, K. Rahimi, M. B. Menhaj, “Maximizing Output Power of a Solar Panel via Combination of Sun Tracking and Maximum Power Point Tracking by Fuzzy Controllers“, International Journal of Photoenergy, vol, Article ID 312580, 13,2010 pages.https://doi.org/10.1155/2010/312580.

[10] Dr-Amjad Ali, Khalid Almutairi, “Investigation of MPPT Techniques Under Uniform and Non-Uniform Solar Irradiation Condition-A Retrospection“,IEEE Access 8(99):127368-127392, DOI:

Journal of Information Systems Engineering and Management
2025, 10(49s)
e-ISSN: 2468-4376
https://www.jisem-journal.com/

Research Article

10.1109/ACCESS.2020.3007710.

[11] Almeida D, Pasupuleti J, Ekanayake J, "Comparison of Reactive Power Control Techniques for Solar PV Inverters to Mitigate Voltage Rise in Low-Voltage Grids ", Electronics; 10(13):1569.2021, https://doi.org/10.3390/electronics10131569.